Title

Cardiac Repair in a Porcine Model of Acute Myocardial Infarction with Human Induced Pluripotent Stem Cell-Derived Cardiovascular Cells

Journal

Cell Stem Cell, 15(6)

ISSN

1934-5909

Authors

Ye, Lei
Chang, Ying-Hua
Xiong, Qiang
et al.

Publication Date

2014-12-01

DOI

10.1016/j.stem.2014.11.009

Peer reviewed

Published in final edited form as:
Cell Stem Cell. 2014 December 4; 15(6): 750–761. doi:10.1016/j.stem.2014.11.009.

Cardiac repair in a porcine model of acute myocardial infarction with human induced pluripotent stem cell-derived cardiovascular cell populations

Lei Ye[1,2], **Ying-Hua Chang**[3], **Qiang Xiong**[1], **Pengyuan Zhang**[1], **Liying Zhang**[1], **Porur Somasundaram**[1], **Mike Lepley**[2,4], **Cory Swingen**[1], **Liping Su**[1], **Jacqueline S. Wendel**[5], **Jing Guo**[1], **Albert Jang**[6], **Daniel Rosenbush**[1], **Lucas Greder**[2], **James R. Dutton**[2], **Jianhua Zhang**[7], **Timothy J. Kamp**[3,7], **Dan S. Kaufman**[2,4], **Ying Ge**[3,8], and **Jianyi Zhang**[1,2,5,6]

[1]Division of Cardiology, Department of Medicine, University of Minnesota, Minneapolis, MN, 55455, USA

[2]Stem Cell Institute, University of Minnesota, Minneapolis, MN, 55455, USA

[3]Department of Cell and Regenerative Biology, University of Wisconsin, Madison, WI, 53705, USA

[4]Division of Hematology, Oncology, and Transplantation, Department of Medicine, University of Minnesota, Minneapolis, MN, 55455, USA

[5]Department of Biomedical Engineering, University of Minnesota, Minneapolis, MN, 55455, USA

[6]Department of Electrical and Computer Engineering, University of Minnesota, Minneapolis, MN, 55455, USA

[7]Department of Medicine, University of Wisconsin, Madison, WI, 53705, USA

[8]Department of Chemistry, University of Wisconsin, Madison, WI, 53706, USA

Summary

Human induced pluripotent stem cells (hiPSCs) hold promise for myocardial repair following injury, but preclinical studies in large animal models are required to determine optimal cell preparation and delivery strategies to maximize functional benefits and to evaluate safety. Here, we utilized a porcine model of acute myocardial infarction (MI) to investigate the functional impact of intramyocardial transplantation of hiPSC-derived cardiomyocytes, endothelial cells, and smooth muscle cells, in combination with a 3D fibrin patch loaded with insulin growth factor (IGF)-encapsulated microspheres. hiPSC-derived cardiomyocytes integrated into host myocardium and generated organized sarcomeric structures, and endothelial and smooth muscle cells contributed to host vasculature. Tri-lineage cell transplantation significantly improved left

Corresponding author: Jianyi (Jay) Zhang, MD., PhD., Professor of Medicine and Biomedical Engineering, Department of Medicine/ Cardiology, University of Minnesota Medical School, Minneapolis, MN 55455, zhang047@umn.edu.

CONFLICT OF INTERESTS: NA

ventricular function, myocardial metabolism, and arteriole density, while reducing infarct size, ventricular wall stress and apoptosis without inducing ventricular arrhythmias. These findings in a large animal MI model highlight the potential of utilizing hiPSC-derived cells for cardiac repair.

Keywords

human induced pluripotent stem cells; cell therapy; metabolism; myocardial infarction; heart

INTRODUCTION

Human induced pluripotent stem cells (hiPSC) are promising therapeutic agents that can potentially generate an unlimited range and quantity of clinically relevant cell types that are not rejected by the patient's immune system. Several studies have reported generation of cardiomyocytes from hiPSCs (Burridge et al., 2012), and transplantation of these cells into rodent models of MI have suggested they may provide functional benefit (Caspi et al., 2007; Laflamme et al., 2007; Shiba et al., 2012; van Laake et al., 2008). In a guinea pig model of cardiac injury, transplanted human embryonic stem cell-derived cardiomyocytes (hESC-CMs) showed electric coupling to native myocardium (Shiba et al., 2012). However, preclinical studies in large animal models of MI are necessary to fully evaluate the therapeutic potential of this approach and to empirically determine the optimal combination of cell types, supplementary factors, and delivery methods to maximize efficacy and stringently assess safety (Cibelli et al., 2013). To this end, Chong et al. utilized a non-human primate model of myocardial ischemia, injecting one billion hESC-CMs into the hearts of macaques with MI injury, and finding extensive evidence of engraftment, remuscularization, and electromechanical synchronization two to seven weeks following transplantation (Chong et al., 2014). Despite these promising findings, telemetric electrocardiographic (ECG) evaluation demonstrated ventricular arrhythmias in some treated animals, suggesting further investigation of optimal cell quantities and delivery approaches is warranted.

Currently, poor engraftment of transplanted cardiomyocytes presents a significant barrier to transplantation-based approaches for myocardial cell therapy. In vitro studies strongly suggest that myocytes survive better when co-cultured with endothelial cells (EC) than when cultured alone (Lan et al., 2006; Xiong et al., 2012). Co-administration of ECs could enhance CM survival and benefit left ventricular (LV) myocardial perfusion, metabolism and contractile activity through release of signaling molecules such as nitric oxide, vascular endothelial growth factor (VEGF), and insulin growth factor (IGF), which has also been shown to inhibit apoptosis (Davis et al., 2006) (Brutsaert, 2003; Hsieh et al., 2006). Consistent with this hypothesis, we recently demonstrated that transplantation of hiPSC-derived ECs (hiPSC-ECs) and smooth muscle cells (hiPSC-SMCs) into ischemic porcine myocardial tissue contributes to improvements in perfusion, wall stress, and cardiac performance (Xiong et al., 2012); however, myocardial repair and functional improvements may be even more extensive if primary force-producing myocardial cells are included in the population of transplanted cells.

In the present study, we injected three hiPSC-derived cell types (hiPSC-CMs, -ECs, and -SMCs) directly into injured hearts in a porcine large animal model of acute myocardial infarction. Cells were co-injected through an epicardial fibrin patch that provided prolonged release of the pro-survival factor insulin-like growth factor 1 (IGF-1), and cell engraftment and functional outcomes were evaluated. Our results show engraftment of cells from all three lineages at the site of injury, for at least 4 weeks after injection. This was accompanied by improvements in myocardial wall stress, metabolism, and contractile performance, and, importantly, did not lead to the development of ventricular arrhythmias. Together, these findings show that co-administration of multiple hiPSC-cardiovascular lineage cell populations promotes myocardial repair in large-animal models of MI.

RESULTS

Differentiation of hiPSCs into cardiac-lineage CMs, ECs, and SMCs

HiPSCs were reprogrammed from human dermal fibroblasts and engineered to express eGFP (Figure S1) and differentiated into CMs via the Sandwich method (Zhang et al., 2012). Isolated areas of contracting cells typically appeared on day seven of differentiation (Movies S1–S3) and were collected one week later for purification via a micro-dissection and preplating method. Expression of cardiac-specific proteins in differentiated hiPSC-CMs was evaluated on Day 30 after cells started contracting. Nearly all hiPSC-CMs expressed slow myosin heavy chain, α-sarcomeric actin (Figure 1A), and the cardiac-specific myofilament cTnT (Figure 1B). Approximately 20–30% of the hiPSC-CMs expressed the 2v isoform of myosin light chain (MLC2v) (Figure 1B, middle), which is found only in ventricular CMs, and cardiac connexin-43 was present at numerous points of contact between adjacent cells (Figure 1C). The purity of the final hiPSC-CM population was as high as 93% when evaluated via flow cytometry analysis of cTnT expression (Figure 1D–E) and >90% when evaluated via fluorescence immunostaining for cTnT expression (Figure 1F). hiPSC-ECs and -SMCs were generated via established differentiation protocols (Hill et al., 2010; Woll et al., 2008) and expressed EC- and SMC-specific proteins (Figures 1G–1L).

hiPSC-derived cardiac cells engraft and survive following transplantation into a porcine model of myocardial infarction

We then tested our hypothesis that transplantation of three hiPSC-derived cardiac cell types would improve recovery after ischemic myocardial injury in a large-animal model (swine) of ischemia-reperfusion (IR) injury. A total of 92 pigs underwent the IR protocol; 89 pigs survived and were divided into 5 groups (Table S1). Animals receiving CMs, EC, and SMCs (Cell group) or CMs, ECs, SMC, and the fibrin/IGF-1 patch (Cell+Patch group) were injected with 2 million hiPSC-CMs, 2 million hiPSC-ECs, and 2 million hiPSC-SMCs (6 million cells total) directly into the injured myocardium; for animals in the Cell+Patch group, the needle was inserted through an IGF-1–containing fibrin scaffold patch (Figure S2) that had been created over the site of injury. Animals in the Patch group were treated with scaffold patch alone, and both the patch and the cells were withheld from animals in the MI group. Animals in the Sham group underwent all surgical procedures for induction of IR injury, except for the ligation step, and recovered without any experimental treatments.

We then evaluated the engraftment and survival rates of the transplanted cells. Since the transplanted cells were genetically male and engineered to express GFP, while the recipient pigs were female, we performed quantitative PCR (qPCR) assessments for the human Y chromosome. Lineages of surviving cells were determined by staining for expression of the human-specific EC marker CD31 (hiPSC-ECs), for co-expression of GFP and α-smooth-muscle actin (SMA) (hiPSC-SMCs), and for co-expression of GFP and cTnT (hiPSC-CMs).

At four weeks after injury, 4.2±1.1% of transplanted cells survived in animals in the Cells group while 8.97±1.8% survived in the hearts of Cell+Patch animals. In contrast, 3.2±0.4% of the 2 million cells administered to the CM group survived. Substantial proportions of all three transplanted cell types were observed in Cell+Patch hearts: 27.1±5% of surviving transplanted cells were hiPSC-CMs, 34.2±10% were hiPSC-ECs, and 40.5±1% were hiPSC-SMCs. These observations suggest that the IGF-1–containing fibrin patch may have substantially improved the engraftment of all three hiPSC-derived cell lineages. Furthermore, GFP-expressing cells were present in cardiac muscle fibers (Figures 2A), but rarely in fibers composed of porcine cardiomyocytes (Figures S3A–S3D), suggesting that the transplanted hiPSC-CMs may have developed into new muscle fibers rather than incorporating into existing host cardiac muscle. GFP^+ cells were also identified in capillaries and arterioles (Figures 2B–2C), although the proportion of vessels apparently generated directly from transplanted cells was less than 0.1%.

Transplantation of hiPSC-derived cardiac cells improves cardiac function and bioenergetics after MI

Measurements of cardiac function were evaluated one and four weeks after injury and cell transplantation. Left-ventricular ejection fraction (LVEF) was significantly better in Cell +Patch group animals than in MI and Patch animals (Figure 3A) at four weeks. Systolic thickening fractions that reflect regional myocardial contractility, were significantly greater in the infarct zone (IZ) and at the border zone (BZ) of the infarct in hearts from Cell+Patch animals than in MI hearts at both week 1 and week 4 timepoints (Figure 3B). Infarct size was significantly smaller in Cell+Patch hearts than in MI hearts ($p<0.05$) at Week 1, while the difference between Cell+Patch and Patch hearts approached statistical significance ($p=0.051$) (Figure 3C). Measurements of regional wall stress performed 4 weeks after injury were significantly lower in Cell+Patch hearts than in Patch hearts (Figure 3D). Together, these results show that transplantation of multiple hiPSC-derived cardiac lineages, in combination with IGF-1/fibrin patch, improves cardiac function following MI.

We then determined whether these functional improvements in Cell+Patch animals were accompanied by improved myocardial bioenergetics and efficient ATP utilization. Myocardial ATP hydrolysis rates were measured in vivo with the ^{31}P MRS-MST method (Xiong et al., 2013). Measurements were performed at the BZ of the infarct under both baseline and elevated cardiac workstates in response to catecholamine stimulation.

Myocardial PCr/ATP ratios that reflect mitochondrial energetic effciancy, were significantly higher in animals from the Cell+Patch group than in MI animals under baseline conditions (Figure 3E), while the rate of ATP hydrolysis was significantly higher in Cell+Patch group hearts than in MI and Patch hearts during high cardiac workload (Figure 3F); measurements

in Patch and MI animals were similar under both conditions. Collectively, these observations indicate that the transplantation of hiPSC-derived cardiovascular cells improved LV pump function and myocardial energy metabolism while reducing infarct size.

Combined hiPSC-CM and patch treatment does not induce ventricular arrhythmias

Arrhythmogenesis is a primary risk associated with pluripotent cell-derived CM therapy for treatment of cardiac disorders. In a recent study, significant ventricular arrhythmias were detected following transplantation of hESC-CMs in a non-human primate model of MI (Chong et al., 2014). Thus, we examined whether the hiPSC-CM patch transplantation protocol used here might be associated with onset of cardiac arrhythmia. Ischemia-reperfusion injury was induced in 16 pigs who then received the fibrin/IGF-1 patch alone (Patch group), the patch and 10 million hiPSC-CMs (Patch+CMs), or neither experimental treatment (Table S1). ECGs were recorded continuously for 4 weeks afterward using an implantable loop recorder. Severe arrhythmias and ST elevations were observed in all animals during coronary artery occlusion and reperfusion, but no animal in any treatment group developed spontaneous arrhythmia during the four -week follow-up period. Furthermore, no evidence of ventricular tachycardia (VT) or ventricular fibrillation (VF) was induced in response to programmed electrical stimulation (PES) in hearts of Patch+CM group animals, even when the most aggressive stimulation protocol was applied. Thus, the combined Patch+hiPSC-CM administration protocol used for the experiments described in this report does not appear to impair the electromechanical stability of swine hearts.

Transplantation of hiPSC-derived cardiac cells reduces cardiomyocyte apoptosis and stimulates Nkx2.5 expression after IR injury

We next assessed how Cell+Patch treatment improves cardiac function. One possibility is through induction of cytoprotective mechanisms. To evaluate this possibility, we measured apoptosis in the hearts of animals sacrificed three days after IR injury and treatment (Figures 4A–G). At the BZ of the infarct, apoptotic (i.e., $TUNEL^+$) cells were significantly less common in animals from the Cell+Patch group than in MI and Patch animals, both in the total cell population (Figure 4F) and specifically among CMs (i.e., $cTnI^+$ cells) (Figure 4G). Furthermore, the proportion of CMs that expressed Nkx2.5 (Figures 4H–N), which has been shown to protect CMs from oxidative stress (Toko et al., 2002), was significantly greater in Cell+Patch animals than in MI animals at Week 4 ($p<0.05$), and the difference between Cell +Patch and Patch animals approached statistical significance ($p=0.056$), at Week 1 after IR injury (Figure 4N). Nkx2.5 expression in MI hearts increased at Week 4, but remained significantly lower than in Cell+Patch hearts. Thus, transplantation of hiPSC-derived cells increased cell survival during the first few days after IR injury, and is associated with upregulation of Nkx2.5 expression. The decline in apoptosis could also result from improvements in wall stress and decreased fibrosis. Consistently, examination of Masson-Trichrome–stained heart sections from animals sacrificed at week 4 showed thicker subepicardium in the region where the patch was applied (~2.44 mm) than in animals from the Sham (0.16 mm) or MI (0.88 mm) groups (Figure S4).

Transplantation of hiPSC-derived cardiac cells enhance the vasculogenic response to IR injury

Increased angiogenesis could also contribute to improved ventricular function. We therefore assessed whether transplantation of hiPSC-derived cardiac cells promotes angiogenesis in peri-infarct border zone (BZ) of MI hearts. Four weeks after injury, CD31+vascular structures and arterioles that co-expressed CD31 and SMA were significantly greater in the BZ of Cell and Cell+Patch hearts than in the corresponding regions of MI and Patch hearts (Figure 5). Additionally, vascular density was significantly greater in the CM group than in the MI group. Thus, transplantation of the hiPSC-derived cardiac cells promoted neovascularization, likely by inducing paracrine mechanisms in recipient myocardial tissue (Table S2).

The cell and patch treatments may also have delayed the immune response to IR injury. While infiltration of cells expressing the inflammatory marker CD11b (Figures S5A–S5F) peaked three days after injury in the MI group, this was significantly delayed in the IZ and BZ regions of hearts from Cell+Patch animals (Figure S5G). $CD11b^{+}$ cells were significantly more common in Cell+Patch hearts than in MI hearts at week 1 but not at Week 4, while the CM, Cells, and Patch groups showed a statistically non-significant increase at weeks one and four, suggesting a delayed host immune response following cell transplantation, possibly reducing immune rejection and increasing engraftment and survival of hiPSC-derived cells.

Paracrine factor release from the hiPSC-derived cells

This increase in angiogenesis observed following Cell+Patch treatment could be due to release of paracrine factors, as suggested by studies showing endothelial cells promote cardiomyocyte survival (Lan et al., 2006; Xiong et al., 2012). To determine whether hiPSC-derived vascular cells possess cytoprotective effects similar to those previously reported in similar cell types, hiPSC-CMs were cultured under hypoxic conditions in media collected from the hiPSC-derived vascular cells (i.e., conditioned media) or with unconditioned (basal) media. hiPSC-CMs tended to shrink when cultured with unconditioned media but not when cultured with the conditioned media (Figures 5I–5J). Culture in conditioned media was also associated with significant declines in hiPSC-CM apoptosis (Figures 5K–5L, 5N) and in the amount of cytoplasmic leakage of lactate dehydrogenase (LDH) from hiPSC-CMs (Figure 5M). Thus, hiPSC-derived vascular cells appear to release paracrine factors that protect hiPSC-CMs from hypoxic injury.

We then performed protein array analysis to identify paracrine factors that may be responsible for these in-vitro cytoprotective effects and that might induce repair mechanisms in injured myocardial tissue. A total of 21 factors were detected, and their expression was confirmed in hiPSC-CMs, as well as hiPSC-derived vascular cells (Table S2). Several of the identified factors are known to impede apoptosis (angiogenin, angiopoietin, IL-6, MMP-1, PDGF-BB, TIMP-1, uPAR, and VEGF), induce cell migration or homing (angiogenin, angiopoietin, IL-8, MCP-1, MCP-3, MMP-9, uPAR, VEGF), and promote cell division (angiogenin, angiopoietin, PDGF-BB, VEGF), suggesting multiple paracrine mechanisms through which hiPSC-ECs and –SMCs could promote CM survival and cardiac repair.

Myocardial protein expression after IR injury and cell therapy

Understanding changes in the expression profile of myocardial proteins will help reveal the molecular mechanisms underlying improvements in left ventricular function associated with cell therapy. To provide further insights into these mechanisms, we performed a quantitative proteomics analysis on LV tissues from SHAM hearts and from MI hearts that were treated with or without hiPSC-derived vascular cells (which have both hiPSC-ECs and -SMCs) after IR injury (Figures S6). We confidently identified 66 proteins whose expression pattern was altered in MI hearts but fully or partially restored to normal after cell transplantation (Figure 6). Thus, the functional benefits associated with cell therapy appear to be accompanied by a recovery of the myocardial protein expression profile of the recipient hearts.

DISCUSSION

The present study is among the first to evaluate the combined administration of three hiPSC-derived cardiovascular lineage cells in a large-animal model of ischemic myocardial injury. Our results indicate that when hiPSC-CM, -SMC and -EC injection is performed through a fibrin patch that has been created over the injection site and contains gelatin microspheres that release IGF-1 into the surrounding tissue, the engraftment rate of the transplanted cells can be as high as 8.97±1.8% four weeks after transplantation, which is ~20 fold greater than the engraftment rate observed when adult swine progenitor cells were evaluated in the same animal model (Zeng et al., 2007). Our results also demonstrate that the transplanted cells developed into functioning CMs and vascular cells, and that the combination of hiPSC-CM, -EC, and -SMC injection with patch application led to significant improvements in LV wall stress, infarct size, systolic thickening fraction, vascular density, and ATP turnover rate. These findings are consistent with the concept that the severity of LV functional decline and structural remodeling is proportional to scar size (Pfeffer and Braunwald, 1990), and that LV dilatation and hypertrophy are exacerbated as increases in systolic wall stress propagate from the IZ and BZ to the adjacent myocardium (Pfeffer and Braunwald, 1990).

Previous attempts to isolate hiPSC- or hESC-derived CMs have been only moderately successful. Xu et al., (Xu et al., 2006) used a method based on Percoll separation and cardiac body formation to obtain hESC-CMs, but just 35–66% of the isolated cells expressed slow myosin heavy chain or cTnT, suggesting the purity of the obtained population would not be sufficient for use in large-animal models. With the differentiation protocol (Zhang et al., 2012) used here, 68% of the differentiated cells expressed cTnT, and the purity was subsequently increased to >90% via micro-dissection and preplating, yielding a total of 3–4 million hiPSC-CMs per well. This yield and purity is sufficient for experiments in large animal models and supports the feasibility of potential clinical trials.

One of the primary factors limiting the effectiveness of cell therapy is the low proportion of transplanted cells that survive in the recipient heart a few weeks following transplantation (Beauchamp et al., 1999; Qu et al., 1998; Tang et al., 2010; Zeng et al., 2007). Co-administration of a cytoprotective agent, such as IGF-1, can improve cell survival rate (Davis et al., 2006; Li et al., 1997; Wang et al., 1998), but the administered cells may still be lost following re-establishment of blood flow or be forced out of the myocardium along the needle track by high pressure during systolic contraction. Notably, a considerably higher

rate of engraftment was observed in hearts from the Cell+Patch group, which was 2-fold greater than the rate observed in Cell group hearts, ~2.5-fold greater than observed in CMs hearts, and ~4-fold greater than when only hiPSC-derived ECs and SMCs were incorporated into a growth-factor enriched patch (Shimizu et al., 2002; Xiong et al., 2013). This can be partially attributed to the fibrin patch itself, as the patch forms a physical barrier preventing ejection of the cells into the epicardial space while providing a prolonged IGF-1 supply to promote cell survival.

The overall engraftment rate for the three cell populations administered to Cell+Patch animals was ~9% and the proportion of cells that expressed EC-, SMC-, or CM-specific markers are ~34%, ~40%, and ~27%, respectively. Substantial engraftment of stem cell–derived CMs has also been observed in a primate model of postinfarction LV remodeling (Chong et al., 2014): ~2% of the LV was composed of engrafted cells, but the precise engraftment rate could not be calculated because the engrafted cells were not counted. However, macaque hearts are ~1/6 the size of human hearts (37–52 g versus ~300 g), which contain ~3 billion CMs, and ~70% of cardiac mass is contained in the LV; thus, the LVs of the animals used in the primate study likely contained ~350 million CMs, ~7 million of which (i.e., 2% of 350 million) were the transplanted hESC-CMs. Since 1 billion hiPSC-CMs were administered to each macaque, the engraftment rate appears to have been ~0.7%, which is consistent with other rates reported in the literature (Zeng et al., 2007) and ~10-fold lower that the rate of hiPSC-CM engraftment observed in the Cell+Patch animals in the present study.

One of the most critical concerns associated with cardiac cell therapy is the development of arrhythmogenic complications. The study by Chong, et al., (Chong et al., 2014) illustrates that transplantation of human CMs to large animal post-MI models can unmask potential arrhythmic complications which are not observed in comparable small animal models (Shiba et al., 2012). All the monkeys studied by Chong et al., (Chong et al., 2014) that received hESC-CMs developed spontaneous arrhythmia during the EKG follow-up evaluations. In the present study, we used a strategy of a smaller cell dose and aiming at mobilization of the endogenous cardiac progenitors, which we have reported earlier (Zeng et al., 2007) (Xiong et al., 2013). We used a 100-fold lower dose of hiPSC-CMs compared to Chong's report, and found no increase of spontaneous or PES-induced arrhythmia in any of the animals received cell therapy. The remarkably better electromechanical stability achieved with our approach may be attributable, in part, to the smaller cell dose used (10 million versus 1 billion) and targeting the cytokine associated mobilization of the endogenous progenitors (Xiong et al., 2013; Zeng et al., 2007). Electromechanical connectivity may be more extensive between native tissues and tissues generated through endogenous repair mechanisms than between native tissues and large piece of cardiac tissue that develop directly from the engrafted cells. Co-administration of ECs that have been linked to the regulation of cardiovascular physiology (Brutsaert, 2003; Hsieh et al., 2006) and could have further improved myocardial recovery primarily through the enhancement of cytokine associated mechanisms. These data also indicate that strategies designed to promote the paracrine effect of transplanted CMs and ECs maybe be more desirable in cardiac cell therapy.

Transplantation of hiPSC-derived cells was also associated with increases in the expression of Nkx2.5 in host cardiomyocytes, which is known to protect cardiomyocytes from oxidative damage (Toko et al., 2002). Furthermore, myocardial perfusion is maintained by the regulatory activity of small resistant vessels (Frame and Sarelius, 1993), so the significant increase in myocardial arteriole density observed in the BZ of Cell+Patch–treated hearts also likely contributed to declines in apoptosis and to the preservation of contractile function. The increase in arteriole density appears to have occurred through the sprouting of pre-existing microvessels in the BZ of the treated hearts, because nearly all of the vessels were GFP negative. The increase in arteriole density was also accompanied by a significant improvement in the myocardial ATP turnover rate (Figure 3F). The calculated rate, which incorporates the rates associated with all enzymatic processes that support contraction and relaxation as well as the rates generated by rapid near-equilibrium enzymes, was markedly reduced at the BZ of infarction in MI hearts, while measurements under high workload conditions were significantly greater in Cell+Patch animals than in animals from either the MI or Patch group.

Cyclosporine was administered to animals from all treatment groups to reduce the likelihood of immune rejection in animals treated with the hiPSC-derived cells. Nevertheless, assessments of $CD11b^{+}$ cell density suggest that the immune response was both elevated and delayed in Patch, CM, CM+EC+CM, and Cell+Patch animals (though the increase was significant in only the Cell+Patch group). Both the patch and the transplanted cells could have contributed to this increase, because the patch was created by combining fibrin with thrombin, which is known to amplify the inflammation induced by ischemia (Chen and Dorling, 2009), and because the transplanted cells released inflammatory cytokines such as MCP-1 and IL-6. Notably, IL-6 production was 8-fold and 20-fold higher in hiPSC-ECs than in hiPSC-CMs or hiPSC-SMCs, respectively. Future study may be required to find an optimal dosage of cyclosporine or addition of other immuno suppression regimen, such as FK506, to minimize the immune rejection and achieve higher cell engraftment rate.

In conclusion, the studies described in this report are the first to evaluate the combined use of hiPSC-ECs, -SMCs, and -CMs in a porcine model of ischemia reperfusion myocardial injury. Our results demonstrate that when the enhanced cell delivery was achieved by an IGF-1 containing fibrin patch, the engraftment rate was remarkably greater than achieved with any other delivery method used in the porcine IR model (Zeng et al., 2007). Furthermore, the combination of all three cell types with extended, patch-mediated IGF-1 administration was associated with significant improvements in myocardial wall stress, apoptosis, arteriole density, metabolism, and contractile function. Collectively these observations support the feasibility of future mechanistic studies of hiPSC-derived cardiac cells in large animal models. Studies with longer follow-up periods will also be needed to ensure that the benefits of treatment are maintained and to fully characterize any potential adverse effects that may be associated with this promising therapeutic modality.

EXPERIMENTAL PROCEDURES

Generation and characterization of hiPSC-derived cardiac cells

The hiPSC-CMs, -SMCs, and -ECs used in this study were generated from two hiPSC lines: DriPS16 (Cell+Patch group) and GRiPS (for the CM and CM+EC+SMC groups). Both hiPSC lines were reprogrammed from male, human, neonatal, dermal fibroblasts by transfecting cells with either lentivirus (DriPS16) or Sendai viruse (GRiPS) coding for OCT4, SOX2, KLF4, and C-MYC and then engineered to constitutively express green fluorescence protein (GFP). Cells were cultured in hiPSC growth medium with irradiated mouse embryonic fibroblasts and passaged every 6–7 days (Wilber et al., 2007).

hiPSCs were differentiated into ECs and SMCs as described previously (Hill et al., 2010; Woll et al., 2008). hiPSC-ECs were characterized via the expression of CD31, CD144, and vWF-8 (Xiong et al., 2012). hiPSC-SMCs were characterized via the expression of α-smooth muscle actin (SMA), SM22, and calponin.

In vitro cytoprotection assays are detailed in Supplemental Experimental Procedures

Paracrine factor release from cultured hiPSC-CMs, ECs and SMCs hiPSC-CMs (3.5×10^5) and hiPSC-SMCs (3.5×10^5) were cultured in 6-well plates, washed 3 times with DPBS, and then cultured in 1 mL RPMI basal medium; hiPSC-ECs (4×10^5) were cultured in 1 mL EBM2 basal medium. The medium was collected 48 hours later and analyzed with the Human Angiogenesis Antibody Array G1 Array (RayBiotech, USA). Measurements were corrected for background signals via control assessments with basal media that had been exposed to identical conditions.

Synthesis of IGF-containing microspheres and patch manufacture are detailed in Supplemental Experimental Procedures.

Porcine IR injury model and treatment

Experiments were performed in female Yorkshire swine (~13 kg, 45 days of age, Manthei hog farm, Elk River, MN, USA) (Xiong et al., 2012). The experimental protocol was approved by the IACUC of the University of Minnesota, and all experimental procedures were performed in accordance with the Animal Use Guidelines of the University of Minnesota and consistent with the National Institutes of Health *Guide for the Care and Use of Laboratory Animals* (NIH publication No 85–23).

A total of 108 pigs underwent the ischemia reperfusion (IR) protocol (Table S1). Ninety-two pigs were used in the first part of the study: 2 pigs died of ventricular fibrillation during occlusion, and 1 died of cardiac arrhythmia one week after IR injury while the MRI data were being collected. The remaining 89 pigs were divided into 6 groups. Animals in the CM +EC+SMC and Cell+Patch groups were treated by injecting 2 million hiPSC-CMs, 2 million hiPSC-ECs, and 2 million hiPSC-SMCs (6 million cells total) directly into the injured myocardium; for animals in the Cell+Patch group, the needle was inserted through an IGF-1–containing fibrin patch that had been created over the site of injury. Animals in the Patch group were treated with the IGF-1–containing patch alone, and both the patch and the

cells were withheld from animals in the MI group. Animals in the SHAM group underwent all surgical procedures for the induction of IR injury except for the ligation step and recovered without any of the experimental treatments. 16 pigs were used in loop recorder study. The Patch+CM group used in the arrhythmogenesis experiments exposed to a protocol of fibrin patch enhanced delivery of ten million hiPSC-CMs on surface of the injured myocardium (Table S1).

Patch application was performed by suspending 5 mg of microspheres (loaded with 2.5 μg IGF-1) in 1 mL fibrinogen solution (25 mg/mL); then, the fibrinogen solution was co-injected with 1 mL thrombin solution (80 NIH units/mL, supplemented with 2 μL 400 mM $CaCl_2$ and 200 mM ε-aminocaproic acid) into a 2.3-cm diameter plastic ring that had been placed on the epicardium of the infarcted region to serve as a mold for the patch; the mixture usually solidified within 30 seconds (Xiong et al., 2012). Cells were suspended in 1 mL MEM and administered via 10 intramyocardial injections (0.1 mL/injection).

Cardiac MRI and MR Spectroscopy are detailed in Supplemental Experimental Procedures

The ECG monitoring and programmed electro-stimulation physiology studies

The implantable loop recorders (Medtronic-Reveal, MN, USA) were placed in the left paraspinal area inferior to the angle of the scapula in the subcutaneous plane. It was sutured in the place where the best electrograms were obtained and there was no evidence of myopotential noise. It was programmed in the conventional manner to document VT and asystole. The loop recorder was interrogated at the time of explantation when the animals were sacrificed 4 weeks after the cell therapy.

The programmed electro-stimulation physiology studies (PES study) were done at the time of sacrifice in four weeks. The PES study was done from the epicardium in an open chest fashion. The PES study was done from two sites: one close to the infarct and one remote from the infarct. The study was done with a Medtronic screw lead in the epicardium and the Bard system was used for stimulation. It was done at two cycle lengths at 400 ms and 300 ms drive trains. Four additional stimuli were given till effective refractory period (ERP) was reached or 160 ms.

hiPSC-EC, -SMC, and -CM engraftment rate and immunohistochemical evaluations are detailed in Supplemental Experimental Procedures

Materials and methods for proteomics are detailed in Supplemental Experimental Procedures.

Statistical analysis

Results are presented as mean±standard error of the mean (SEM). Comparisons among groups were analyzed for significance with one-way analysis of variance (ANOVA). A value of $p<0.05$ was considered significant. Results identified as significant via ANOVA were re-analyzed with the Tukey correction. Statistical analyses were performed with SPSS software (version 20).

Supplementary Material

Refer to Web version on PubMed Central for supplementary material.

Acknowledgments

The authors would like to thank W. Kevin Meisner, Ph.D., E.L.S., for his editorial assistance. This work was supported by US Public Health Service grants NIH RO1s, HL UO1 100407, HL UO1 099773, and P41RR08079.

REFERENECES

Beauchamp JR, Morgan JE, Pagel CN, Partridge TA. Dynamics of myoblast transplantation reveal a discrete minority of precursors with stem cell-like properties as the myogenic source. The Journal of cell biology. 1999; 144:1113–1122. [PubMed: 10087257]

Brutsaert DL. Cardiac endothelial-myocardial signaling: its role in cardiac growth, contractile performance, and rhythmicity. Physiological reviews. 2003; 83:59–115. [PubMed: 12506127]

Burridge PW, Keller G, Gold JD, Wu JC. Production of de novo cardiomyocytes: human pluripotent stem cell differentiation and direct reprogramming. Cell stem cell. 2012; 10:16–28. [PubMed: 22226352]

Caspi O, Huber I, Kehat I, Habib M, Arbel G, Gepstein A, Yankelson L, Aronson D, Beyar R, Gepstein L. Transplantation of human embryonic stem cell-derived cardiomyocytes improves myocardial performance in infarcted rat hearts. Journal of the American College of Cardiology. 2007; 50:1884–1893. [PubMed: 17980256]

Chen D, Dorling A. Critical roles for thrombin in acute and chronic inflammation. Journal of thrombosis and haemostasis: JTH. 2009; 7(Suppl 1):122–126. [PubMed: 19630783]

Chong JJ, Yang X, Don CW, Minami E, Liu YW, Weyers JJ, Mahoney WM, Van Biber B, Cook SM, Palpant NJ, et al. Human embryonic-stem-cell-derived cardiomyocytes regenerate non-human primate hearts. Nature. 2014; 510:273–277. [PubMed: 24776797]

Cibelli J, Emborg ME, Prockop DJ, Roberts M, Schatten G, Rao M, Harding J, Mirochnitchenko O. Strategies for improving animal models for regenerative medicine. Cell stem cell. 2013; 12:271–274. [PubMed: 23472868]

Davis ME, Hsieh PC, Takahashi T, Song Q, Zhang S, Kamm RD, Grodzinsky AJ, Anversa P, Lee RT. Local myocardial insulin-like growth factor 1 (IGF-1) delivery with biotinylated peptide nanofibers improves cell therapy for myocardial infarction. Proceedings of the National Academy of Sciences of the United States of America. 2006; 103:8155–8160. [PubMed: 16698918]

Frame MD, Sarelius IH. Regulation of capillary perfusion by small arterioles is spatially organized. Circulation research. 1993; 73:155–163. [PubMed: 8508527]

Hill KL, Obrtlikova P, Alvarez DF, King JA, Keirstead SA, Allred JR, Kaufman DS. Human embryonic stem cell-derived vascular progenitor cells capable of endothelial and smooth muscle cell function. Experimental hematology. 2010; 38:246–257. e241. [PubMed: 20067819]

Hsieh PC, Davis ME, Lisowski LK, Lee RT. Endothelial-cardiomyocyte interactions in cardiac development and repair. Annual review of physiology. 2006; 68:51–66.

Laflamme MA, Chen KY, Naumova AV, Muskheli V, Fugate JA, Dupras SK, Reinecke H, Xu C, Hassanipour M, Police S, et al. Cardiomyocytes derived from human embryonic stem cells in pro-survival factors enhance function of infarcted rat hearts. Nature biotechnology. 2007; 25:1015–1024.

Lan CC, Wu CS, Chiou MH, Hsieh PC, Yu HS. Low-energy helium-neon laser induces locomotion of the immature melanoblasts and promotes melanogenesis of the more differentiated melanoblasts: recapitulation of vitiligo repigmentation in vitro. The Journal of investigative dermatology. 2006; 126:2119–2126. [PubMed: 16691191]

Li Q, Li B, Wang X, Leri A, Jana KP, Liu Y, Kajstura J, Baserga R, Anversa P. Overexpression of insulin-like growth factor-1 in mice protects from myocyte death after infarction, attenuating ventricular dilation, wall stress, and cardiac hypertrophy. The Journal of clinical investigation. 1997; 100:1991–1999. [PubMed: 9329962]

Pfeffer MA, Braunwald E. Ventricular remodeling after myocardial infarction. Experimental observations and clinical implications. Circulation. 1990; 81:1161–1172. [PubMed: 2138525]

Qu Z, Balkir L, van Deutekom JC, Robbins PD, Pruchnic R, Huard J. Development of approaches to improve cell survival in myoblast transfer therapy. The Journal of cell biology. 1998; 142:1257–1267. [PubMed: 9732286]

Shiba Y, Fernandes S, Zhu WZ, Filice D, Muskheli V, Kim J, Palpant NJ, Gantz J, Moyes KW, Reinecke H, et al. Human ES-cell-derived cardiomyocytes electrically couple and suppress arrhythmias in injured hearts. Nature. 2012; 489:322–325. [PubMed: 22864415]

Shimizu T, Yamato M, Isoi Y, Akutsu T, Setomaru T, Abe K, Kikuchi A, Umezu M, Okano T. Fabrication of pulsatile cardiac tissue grafts using a novel 3-dimensional cell sheet manipulation technique and temperature-responsive cell culture surfaces. Circulation research. 2002; 90:e40. [PubMed: 11861428]

Tang XL, Rokosh G, Sanganalmath SK, Yuan F, Sato H, Mu J, Dai S, Li C, Chen N, Peng Y, et al. Intracoronary administration of cardiac progenitor cells alleviates left ventricular dysfunction in rats with a 30-day-old infarction. Circulation. 2010; 121:293–305. [PubMed: 20048209]

Toko H, Zhu W, Takimoto E, Shiojima I, Hiroi Y, Zou Y, Oka T, Akazawa H, Mizukami M, Sakamoto M, et al. Csx/Nkx2–5 is required for homeostasis and survival of cardiac myocytes in the adult heart. The Journal of biological chemistry. 2002; 277:24735–24743. [PubMed: 11889119]

van Laake LW, Passier R, Doevendans PA, Mummery CL. Human embryonic stem cell-derived cardiomyocytes and cardiac repair in rodents. Circulation research. 2008; 102:1008–1010. [PubMed: 18436793]

Wang L, Ma W, Markovich R, Chen JW, Wang PH. Regulation of cardiomyocyte apoptotic signaling by insulin-like growth factor I. Circulation research. 1998; 83:516–522. [PubMed: 9734474]

Wilber A, Linehan JL, Tian X, Woll PS, Morris JK, Belur LR, McIvor RS, Kaufman DS. Efficient and stable transgene expression in human embryonic stem cells using transposon-mediated gene transfer. Stem Cells. 2007; 25:2919–2927. [PubMed: 17673526]

Woll PS, Morris JK, Painschab MS, Marcus RK, Kohn AD, Biechele TL, Moon RT, Kaufman DS. Wnt signaling promotes hematoendothelial cell development from human embryonic stem cells. Blood. 2008; 111:122–131. [PubMed: 17875805]

Xiong Q, Ye L, Zhang P, Lepley M, Swingen C, Zhang L, Kaufman DS, Zhang J. Bioenergetic and functional consequences of cellular therapy: activation of endogenous cardiovascular progenitor cells. Circulation research. 2012; 111:455–468. [PubMed: 22723295]

Xiong Q, Ye L, Zhang P, Lepley M, Tian J, Li J, Zhang L, Swingen C, Vaughan JT, Kaufman DS, et al. Functional consequences of human induced pluripotent stem cell therapy: myocardial ATP turnover rate in the in vivo swine heart with postinfarction remodeling. Circulation. 2013; 127:997–1008. [PubMed: 23371930]

Xu C, Police S, Hassanipour M, Gold JD. Cardiac bodies: a novel culture method for enrichment of cardiomyocytes derived from human embryonic stem cells. Stem cells and development. 2006; 15:631–639. [PubMed: 17105398]

Zeng L, Hu Q, Wang X, Mansoor A, Lee J, Feygin J, Zhang G, Suntharalingam P, Boozer S, Mhashilkar A, et al. Bioenergetic and functional consequences of bone marrow-derived multipotent progenitor cell transplantation in hearts with postinfarction left ventricular remodeling. Circulation. 2007; 115:1866–1875. [PubMed: 17389266]

Zhang J, Klos M, Wilson GF, Herman AM, Lian X, Raval KK, Barron MR, Hou L, Soerens AG, Yu J, et al. Extracellular matrix promotes highly efficient cardiac differentiation of human pluripotent stem cells: the matrix sandwich method. Circulation research. 2012; 111:1125–1136. [PubMed: 22912385]

Highlights

- Human iPSCs (hiPSCs) were differentiated into three cardiac lineages
- HiPSC-derived cells were transplanted into a porcine model of myocardial infarction
- Transplantation in combination with IGF-1-fibrin patch improves cardiac function

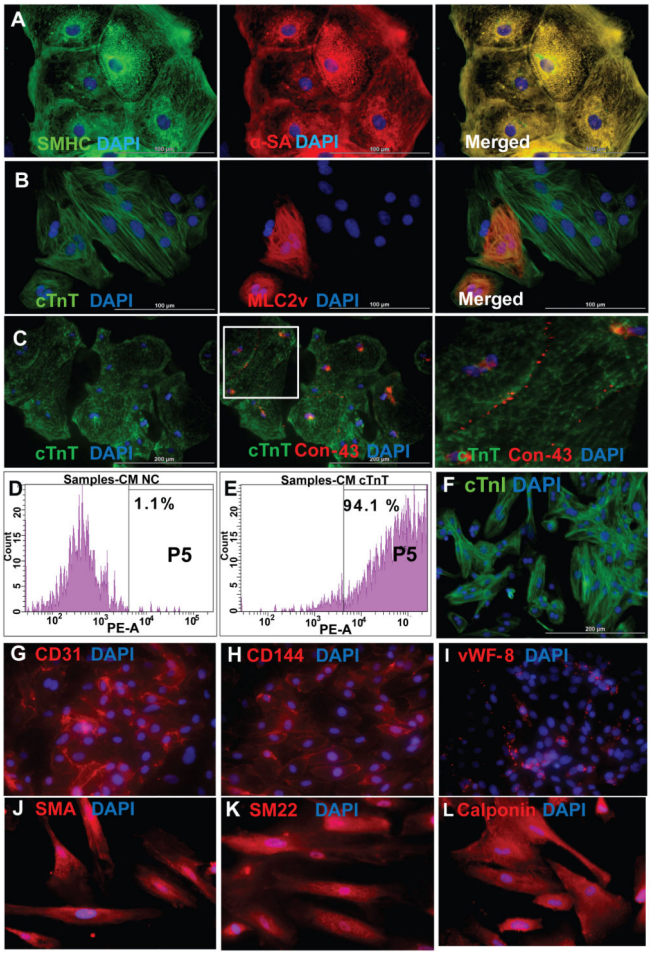

Figure 1. Differentiation of human iPSCs into cardiomyocytes, endothelial cells, and smooth muscle cells

hiPSCs were differentiated into CMs via the Sandwich method (Zhang et al., 2012), and the lineage of the differentiated hiPSC-CMs was confirmed via the expression of **(A)** slow myosin heavy chain (SMHC) and α-sarcomeric actin (α-SA); **(B)** cardiac troponin T (cTnT) and the ventricular- specific cardiomyocyte protein myosin light chain 2v (MLC2v); and **(C)** cTnT and the gap-junction protein connexin-43 (Con-43); nuclei were counterstained with DAPI. The boxed region in the 2nd panel of **C** is shown at higher magnification. **(D–F)** The purity of the hiPSC-CM population was evaluated via flow cytometry analysis of cTnT expression in **(D)** isotype controls and **(E)** purified hiPSC-CMs, and by **(F)** immunofluorescence analysis of cardiac troponin I (cTnI) expression; nuclei were counterstained with DAPI. Bar: 100 μm in A–B, 200 μm in C and F. (See also Movies S1, S2, and S3). hiPSCs were differentiated into ECs and SMCs as described previously (Hill et al., 2010; Woll et al., 2008). **(G–I)** The lineage of the differentiated hiPSC-ECs was confirmed via the expression of **(G)** CD31, **(H)** CD144, and **(I)** vWF-8; and **(J–L)** the lineage of the differentiated hiPSC-SMCs was confirmed via the expression of **(J)** smooth-muscle actin (SMA), **(K)** SM22, and **(L)** calponin. Nuclei were counterstained with DAPI. (Bar: 100 μm in A–B, 200 μm in C and F. Magnification G–L=200x). (See also Figure S1).

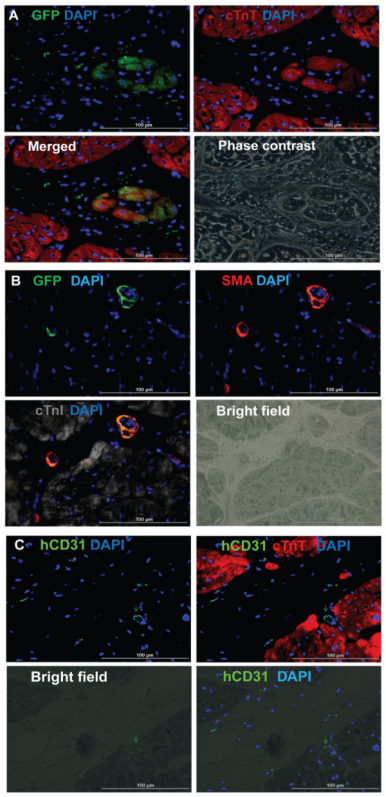

Figure 2. hiPSC-derived cardiac cells engraft and survive after transplantation into the hearts of swine with MI

(A) Engraftment of the injected cells was evaluated in sections stained for the presence of GFP; muscle fibers were visualized via fluorescent immunostaining for cTnT, and nuclei were counterstained with DAPI. The sections displayed in the first three panels of **A** were imaged with a phase-contrast microscope. **(B)** Engrafted cells were identified in arterioles via immunofluorescent staining for the co-expression of GFP and SMA; muscle fibers were visualized via immunofluorescent staining for cTnI and nuclei were counterstained with DAPI. **(C)** Engrafted cells were identified in blood vessels (i.e., capillaries and arterioles) via immunofluorescent staining for the human-specific isoform of CD31; muscle fibers were visualized via cTnT staining and nuclei were counterstained with DAPI. (Bar=100 μm). (See also Figure S3).

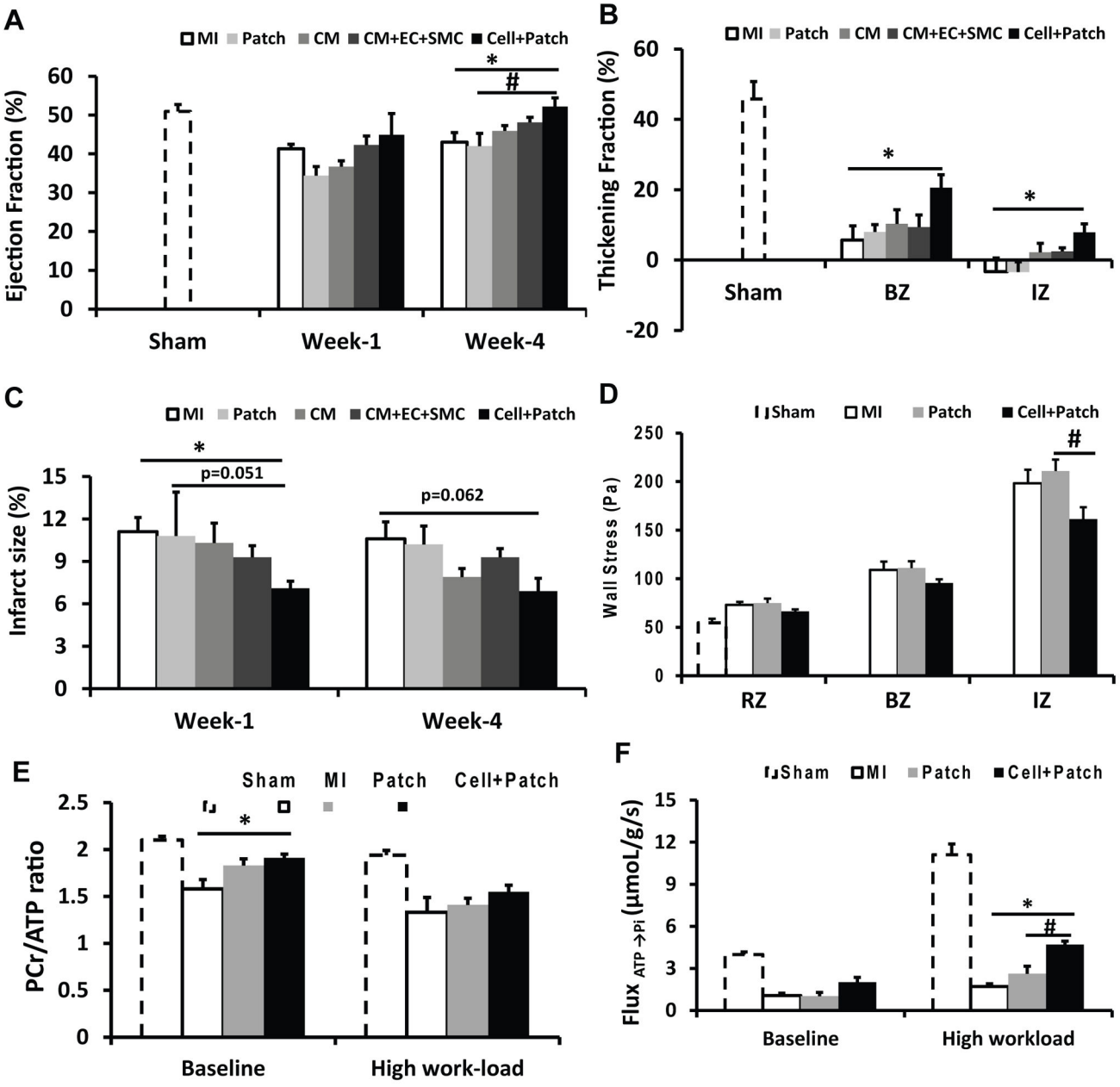

Figure 3. Transplanted hiPSC-derived cardiac lineage cells improve cardiac function

(A) LV ejection fractions were evaluated at Week 1 and Week 4 after MI injury and treatment. **(B)** LV wall systolic thickening fractions in the infarct zone (IZ) and at the border zone (BZ) of ischemia were evaluated at Week 4. **(C)** Infarct sizes were evaluated at Week 1 and Week 4 and expressed as a percentage of the LV surface area. **(D)** LV wall stress in the IZ, in the BZ, and in uninjured regions of the myocardium (i.e., the remote zone [RZ]) was evaluated at Week 4. Four weeks after MI injury and treatment, **(E)** PCr/ATP ratios and **(F)** the ATP hydrolysis rate were determined in the BZ under both baseline conditions and after a high cardiac workload was induced via catecholamine administration; measurements were obtained via a double-saturation ^{31}P MRS-MST protocol. For panels B, D, E, and F,

measurements in Sham animals were performed in regions that corresponded to the site of injury in the other experimental groups. *p<0.05 vs MI; #p<0.05 vs Patch. (See also Figures S2&S4, and Table S1).

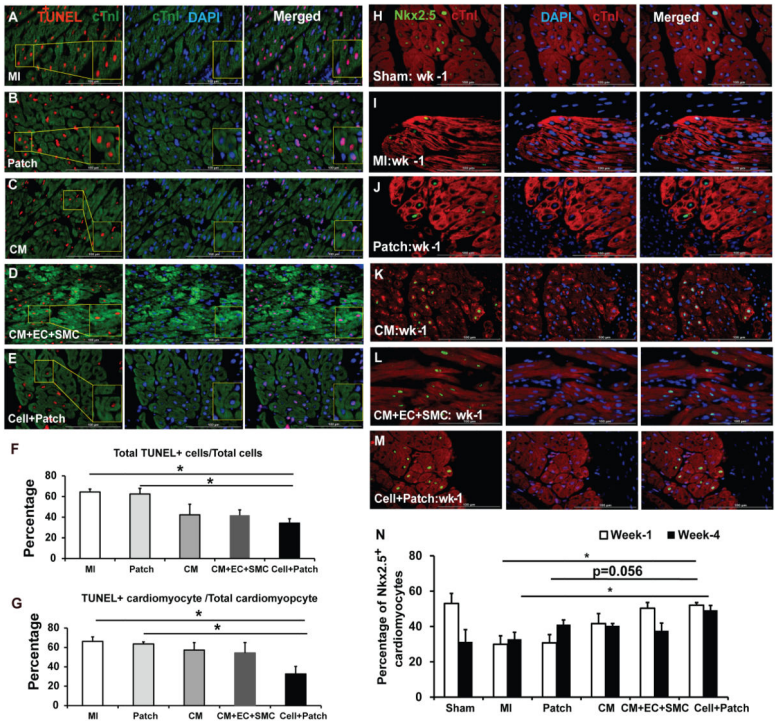

Figure 4. Transplantation of hiPSC-derived cardiac cells reduces cardiomyocyte apoptosis and enhances endogenous cell survival

(A–G) Apoptotic cells were identified in sections from the border zone of infarct in hearts from animals in the **(A)** MI, **(B)** Patch, **(C)** CM, **(D)** CM+EC+SMC, and **(E)** Cell+Patch groups with the TUNEL assay. Muscle fibers were visualized via fluorescent immunostaining for cTnI, and nuclei were counterstained with DAPI; the boxed regions toward the left of panels A, B, C, D, and E are displayed at higher magnification in the boxes at the right of the images. **(F)** Apoptosis was quantified as the percentage of cells that were positive for TUNEL staining. **(G)** Cardiomyocyte apoptosis was quantified as the percentage of cTnI-positive cells that were also positive for TUNEL staining. **(H–N)** NkX2.5 expression was evaluated in sections from the border zone of infarct hearts that compared to Sham operated normal hearts: **(H)** Sham, **(I)** MI, **(J)** Patch, **(K)** CM, **(L)** CM +EC+SMC and **(M)** Cell+Patch. The immunofluorescent staining positives with anti-Nkx2.5 antibody are shown green; muscle fibers were visualized via fluorescent immunostaining for cTnI, and nuclei were counterstained with DAPI. **(N)** The percentage of cardiomyocytes that expressed Nkx2.5 was determined at Week 1 and Week 4 after injury. (*$p<0.05$; bar=100 μm). (See also Table S2)

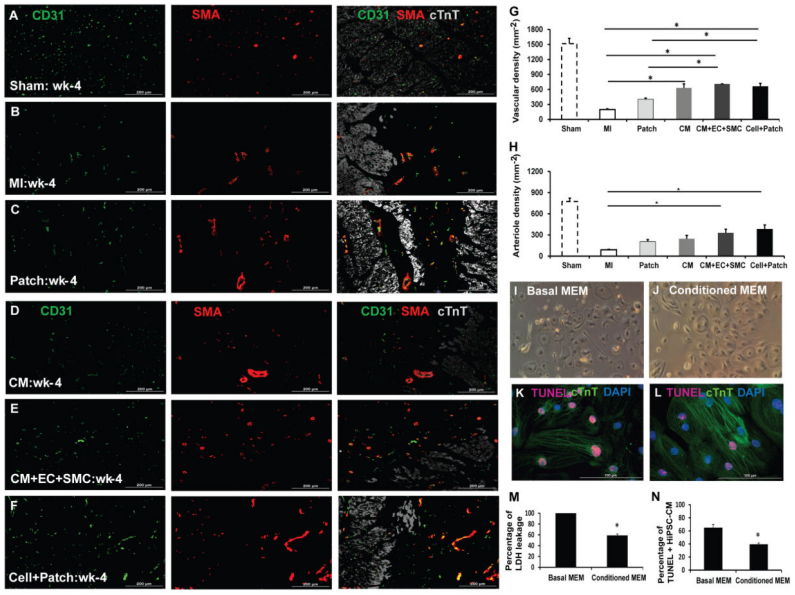

Figure 5. The hiPSC-derived cardiac cells enhance the angiogenic response, and inhibit apoptosis

Vascular density and arteriole density at Week 4 after MI were evaluated in sections from the border zone of infarct in the hearts of animals from the **(A)** Sham, **(B)** MI, **(C)** Patch, **(D)** CM, **(E)** CM+EC+SMC and **(F)** Cell+Patch groups via immunofluorescent staining for CD31 and SMA; muscle fibers were visualized via cTnT staining. **(G)** Vascular density was determined by counting CD31+ vascular structures, and **(H)** arteriole density was determined by counting vascular structures that expressed both CD31 and SMA. (*p<0.05; bar=200μm). **(I–N)** hiPSC-CMs were cultured under hypoxic conditions in **(I)** basal media (Basal MEM) or **(J)** media collected from the hiPSC-derived vascular cells (Conditioned MEM) for 48 hours; then, **(K–L)** apoptotic cells were identified via the TUNEL assay, **(M)** cytotoxicity was quantified via the intensity of lactate dehydrogenase fluorescence observed in the media, and **(N)** apoptosis was quantified as the percentage of cells that were positive for TUNEL staining. *p<0.05 vs basal MEM; magnification: 100x for I&J; bar=100 μm. (See also Figure S5 & Table S2).

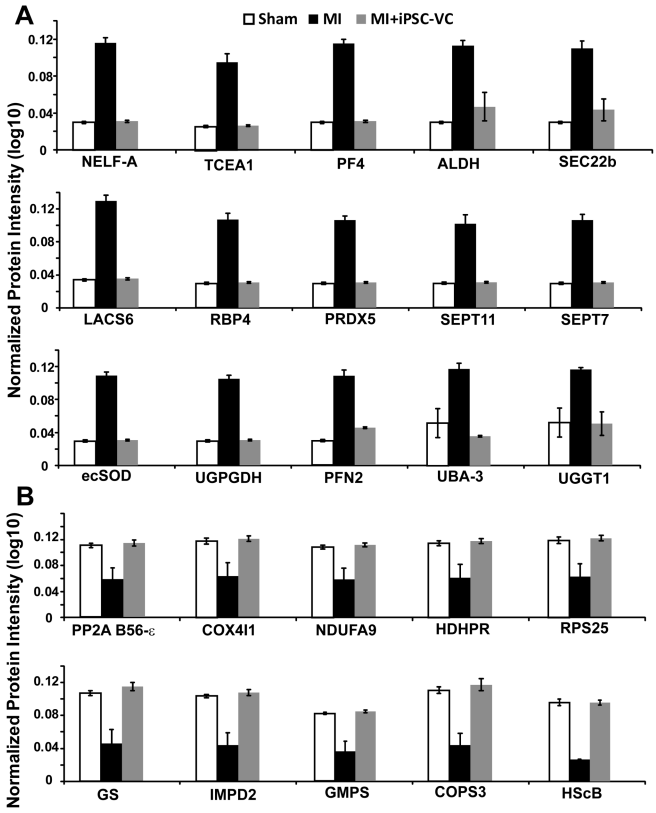

Figure 6. Protein expression levels are significantly altered in MI and partially restored by cell transplantation

Myocardial protein expression profiles were evaluated in animals that had been treated with (MI+iPSC-VC) or without (MI) hiPSC-VC transplantation after experimentally induced MI; control assessments were performed in animals that underwent all surgical procedures for the induction of MI except for the ligation step (SHAM); results are displayed for 25 proteins whose expression levels **(A)** increased or **(B)** decreased after MI and were restored to normal levels by cell therapy. NELF-A, negative elongation factor A; TCEA1, transcription elongation factor A protein 1; PF4, platelet factor 4; ALDH, aldehyde dehydrogenase [mitochondrial]; SEC22b, vesicle-trafficking protein SEC22b; LACS6, long-chain-fatty-acid-CoA ligase 6; RBP4, retinol-binding protein 4; PRDX5, peroxiredoxin-5 [mitochondrial]; SEPT11, septin-11; SEPT7, septin-7; ecSOD, extracellular superoxide dismutase [Cu-Zn]; UGPGDH, UDP-glucose-6-dehydrogenase; PFN2, profiling-2; UBA-3, NEDD8-activating enzyme E1 catalytic subunit; UGGT1, UDP-glucose:glycoprotein glucosyltransferase 1; PP2A B56-ε, serine/threonine-protein phosphatase 2A 56 kDa regulatory subunit ε isoform; COX4I1, cytochrome C oxidase subunit 4 isoform 1, mitochondrial; NDUFA9, NADH dehydrogenase [ubiquinone] 1 α subcomplex subunit 2; HDHPR, dihydropteridine reductase; RPS25, 40S ribosomal protein S25; GS, glutamine synthetase; IMPD2, inosine-5′-monophosphate dehydrogenase 2; GMPS, GMP synthase [glutamine-hydrolyzing]; COPS3, COP9 signlosome complex subunit 3; HScB, iron-sulfur cluster co-chaperone protein HScB [mitochondrial]. (See also Figure S6&S7).